



THE UNIVERSITY *of* EDINBURGH

Edinburgh Research Explorer

Inertia-gravity-wave generation: a geometric-optics approach

Citation for published version:

Aspden, JM & Vanneste, J 2010, Inertia-gravity-wave generation: a geometric-optics approach. in D Dritschel (ed.), IUTAM SYMPOSIUM ON TURBULENCE IN THE ATMOSPHERE AND OCEANS. Springer, NEW YORK, pp. 17-26. DOI: 10.1007/978-94-007-0360-5_2

Digital Object Identifier (DOI):

[10.1007/978-94-007-0360-5_2](https://doi.org/10.1007/978-94-007-0360-5_2)

Link:

[Link to publication record in Edinburgh Research Explorer](#)

Document Version:

Peer reviewed version

Published In:

IUTAM SYMPOSIUM ON TURBULENCE IN THE ATMOSPHERE AND OCEANS

Publisher Rights Statement:

The final publication is available at Springer via http://dx.doi.org/10.1007/978-94-007-0360-5_2.

General rights

Copyright for the publications made accessible via the Edinburgh Research Explorer is retained by the author(s) and / or other copyright owners and it is a condition of accessing these publications that users recognise and abide by the legal requirements associated with these rights.

Take down policy

The University of Edinburgh has made every reasonable effort to ensure that Edinburgh Research Explorer content complies with UK legislation. If you believe that the public display of this file breaches copyright please contact openaccess@ed.ac.uk providing details, and we will remove access to the work immediately and investigate your claim.



Inertia-gravity-wave generation: a geometric-optics approach

J. M. Aspden and J. Vanneste

Abstract The generation of inertia-gravity waves in the atmosphere and oceans is examined using a geometric-optics approach. This approach considers the dynamics of a small-scale wavepacket in prescribed time-dependent, balanced flows. The wavepacket is assumed to be in the so-called wave-capture regime, where the wave intrinsic frequency is negligible compared to the Doppler shift. The dynamics is reduced to a number of ordinary differential equations describing the evolution of the wavepacket position, of its wavevector, and of three scalar fields describing the wavepacket amplitude and polarisation. The approach clearly identifies two classes of wave-generation processes: unbalanced instabilities, associated with linear interactions between inertia-gravity waves, and spontaneous generation, associated with a conversion between vortical and inertia-gravity modes. Applications to simple steady flows and to random-strain models are discussed.

1 Introduction

The dynamics of the atmosphere and ocean is dominated by large-scale, slow motion in nearly geostrophic and hydrostatic balance. Small-scale, fast motion, in the form of inertia-gravity waves can play an important role, however, for instance by transporting momentum or by enhancing mixing. There is, therefore, considerable interest in identifying and quantifying sources of wave activity. Among the source mechanisms, one has proved particularly elusive: the dynamical generation of waves by the evolving balanced flow, often termed spontaneous generation. The difficulty

J. M. Aspden
School of Mathematics and Maxwell Institute, University of Edinburgh, Edinburgh EH9 3JZ, UK,
e-mail: j.m.aspden@sms.ed.ac.uk

J. Vanneste
School of Mathematics and Maxwell Institute, University of Edinburgh, Edinburgh EH9 3JZ, UK,
e-mail: j.vanneste@ed.ac.uk

in capturing this mechanism stems from the smallness of the waves and from the ambiguity that exists in the separation between balanced flow and waves. Nonetheless, several recent results, both numerical and analytical, have clearly demonstrated that spontaneous generation occurs in the small-Rossby-number regime relevant to most of the atmosphere and oceans [22, 17, 23, 24, 18, 16, and references therein]. Asymptotic results, in particular, show that the waves generated in this regime are exponentially small in the Rossby number [22, 20, 21].

The asymptotic work carried so far, relying on the smallness of the Rossby number, has been limited to very simple flows. Here, we propose an alternative approach, based on a spatial-scale separation between waves and balanced flows. This approach can in principle be applied to complex flows, e.g. derived from numerical simulations. It is motivated by the observation that, in many realistic circumstances, the inertia-gravity waves that are generated have a much smaller scale than the balanced flow. A key advantage is that there is no restriction to a large frequency separation between waves and flow, so that the wave generation can be captured when it is at its largest, that is, when relatively short time scales appear. The exponential smallness is of course recovered in the limit of small Rossby number.

2 Geometric-optics approach

The approach we propose is closely related to the geometric-optics approach to stability reviewed in Ref. [7]. This has recently been applied to rotating-stratified flows in [8], where equations equivalent to the ones we now derive have been obtained. The approach considers the evolution of a wavepacket with small wavelength superimposed to a spatially-varying, time-independent basic flow, with velocity $\mathbf{U} = (U, V, 0)$ satisfying $\nabla \cdot \mathbf{U} = 0$. The perturbation fields, in particular the x -component of the velocity, are written in the form

$$u(\mathbf{x}, t) = \hat{u}(\mathbf{x}, t) e^{i\theta(\mathbf{x}, t)/\mu} + \text{c.c.}, \quad (1)$$

where $\mu \ll 1$ characterises the spatial scale separation. Introduction into the three-dimensional Boussinesq equations gives

$$\frac{D\theta}{Dt} = \frac{\partial\theta}{\partial t} + \mathbf{U} \cdot \nabla\theta = 0 \quad (2)$$

at leading order in μ . This equation governs the change in the phase $\theta(\mathbf{x}, t)/\mu$ of wavepackets whose trajectories obey

$$\frac{D\mathbf{x}}{Dt} = \mathbf{U}, \quad (3)$$

that is, they are simply advected by the basic flow. Taking the gradient of (2) leads to

$$\frac{D\mathbf{k}}{Dt} = -(\nabla\mathbf{U})^T \mathbf{k}, \quad (4)$$

where $\mathbf{k} = (k, l, m) = \nabla\theta$ is the wavevector (scaled by μ). This is the standard WKB result for waves whose frequency

$$\omega_0 = \mathbf{U} \cdot \mathbf{k} \quad (5)$$

is entirely associated with the Doppler shift. This is a natural outcome for small-scale inertia-gravity waves, since their intrinsic frequencies

$$\omega_1 = \pm (f^2 m^2 + N^2 (k^2 + l^2))^{1/2} / \kappa, \quad (6)$$

where $\kappa = |\mathbf{k}|$, are formally smaller by a factor μ than the Doppler shift frequency. (Here f and N are the Coriolis and Brunt–Väisälä frequencies, respectively.) The regime considered here, where wavepackets are simply advected by the flow, can be recognised as the wave-capture regime examined in Refs. [3, 4]. Note that this regime is a feature of three-dimensional stratified fluids without analogue in the shallow-water model.

Carrying out the expansion to the next order in μ leads to a system of equations governing the evolution of the complex amplitudes $\hat{u}(\mathbf{x}, t)$, $\hat{v}(\mathbf{x}, t)$, etc. along the wavepacket trajectory. This system can be reduced to a set of three equations for the amplitudes of divergence $\hat{\delta}(\mathbf{x}, t)$, vertical vorticity $\hat{\zeta}(\mathbf{x}, t)$, and potential vorticity $\hat{q}(\mathbf{x}, t)$. Ignoring the effects of the basic-flow buoyancy, these equations reduce to

$$\begin{aligned} \frac{D\hat{\delta}}{Dt} = & \left(\frac{m^2 f}{\kappa^2} + \frac{k^2 + l^2}{\alpha \kappa^2} N^2 + \frac{2m^2}{\kappa^2 (k^2 + l^2)} (kl(\partial_x U - \partial_y V) + l^2 \partial_x V - k^2 \partial_y U) \right) \hat{\zeta} \\ & + \left(\frac{m^2 - k^2 - l^2}{m \kappa^2} (k \partial_z U + l \partial_z V) \right. \\ & \left. - \frac{2m^2}{\kappa^2 (k^2 + l^2)} (kl(\partial_x V + \partial_y U) + l^2 \partial_y V + k^2 \partial_x U) \right) \hat{\delta} - \frac{k^2 + l^2}{\alpha \kappa^2} \hat{q}, \end{aligned} \quad (7)$$

$$\frac{D\hat{\zeta}}{Dt} = -\alpha \hat{\delta}, \quad (8)$$

$$\frac{D\hat{q}}{Dt} = -\hat{\mathbf{u}} \cdot \nabla Q, \quad (9)$$

where $\alpha = f + \Omega + l \partial_z U / m - k \partial_z V / m$, $\Omega = \partial_x V - \partial_y U$, and Q is the potential vorticity of the basic flow. The perturbation velocity field $\hat{\mathbf{u}}$ in (9) is reconstructed from $\hat{\delta}$ and $\hat{\zeta}$ according to

$$\hat{\mathbf{u}} = \frac{1}{k^2 + l^2} \left(il \hat{\zeta} - ik \hat{\delta}, -ik \hat{\zeta} - il \hat{\delta} \right).$$

Equations (3)–(4) and (7)–(9) form a closed system of nine ordinary differential equations governing the position, wavevector and amplitude of the wavepacket. They can be solved for a given, possibly time-dependent, flow to assess whether

perturbations to this flow grow; when the Rossby number is small, the perturbation can further be approximately decomposed into a balanced (or vortical) part and an inertia-gravity-wave part, and the growth of latter implies a mechanism of inertia-gravity-wave generation.

When \mathbf{U} is zero or uniform, the wavevector \mathbf{k} is constant, and the system (7)–(9) is readily solved by letting

$$(\hat{\delta}, \hat{\zeta}, \hat{q}) = \exp(-i\omega_1 t)\mathbf{e}, \quad (10)$$

where \mathbf{e} is a constant three-dimensional vector. The corresponding eigenvalue problem for ω_1 has the three solutions $\omega_1 = 0$ and the two values given in (6) corresponding to the vortical mode and the two inertia-gravity modes, respectively. A non-uniform \mathbf{U} has two consequences for (7)–(9): first, it leads to a time-dependent wavevector \mathbf{k} , and second it directly introduces terms proportional to $\nabla\mathbf{U}$. In general, the ordinary differential equations (3)–(4) and (7)–(9) need to be solved numerically. Some general comments about the behaviour of their solutions can nonetheless be made. We concentrate on the particular case of uniform background potential vorticity, $\nabla Q = 0$, so that the perturbation potential vorticity has a constant amplitude: $\hat{q}(t) = \hat{q}(0)$. The equations (7)–(8) for $\hat{\delta}$ and $\hat{\zeta}$ are then equivalent to the equations governing a linear oscillator with time-dependent frequency and time-dependent forcing. Note that the wavevector enters these equations only through its direction \mathbf{k}/κ

For small Rossby number, the frequency of this oscillator is approximately given by (6); it depends on time on a scale fixed by the Lagrangian time-scale of the strain $\nabla\mathbf{U}$. This gives a good local definition of a Rossby number as the inverse of the product of this time scale by ω_1 . When this number is small, the growth of free-oscillations in $(\hat{\delta}, \hat{\zeta})$ – the mark of inertia-gravity-wave generation – is very weak; in fact, it can be expected to be exponentially small in the Rossby number if the (Lagrangian) time dependence of $\nabla\mathbf{U}$ is smooth (real analytic). Two mechanisms of wave generation can be distinguished. First, for $\hat{q}(0) \neq 0$, the response of $(\hat{\delta}, \hat{\zeta})$ is balanced to all orders in the Rossby numbers; any transient behaviour of $\nabla\mathbf{U}$ does however lead to exponentially small free oscillations. Since these cannot be eliminated by initialisation, the mechanism is one of genuine spontaneous generation [22, 21]; it may be interpreted as a conversion from the vortical mode into the two gravity-wave modes. Note that this conversion is not a conservative one since the background flow provides a source of energy. The second mechanism is active with $\hat{q} = 0$. In this case, the equations for $(\hat{\delta}, \hat{\zeta})$ describe a slowly varying (unforced) oscillator, and the adiabatic invariance of the action, which holds to all orders in the Rossby number, applies; thus, in a transient scenario where \mathbf{U} is uniform as $t \rightarrow \pm\infty$, $(\hat{\delta}, \hat{\zeta})$ can only change by an exponentially small amount. However, if \mathbf{U} remains time dependent, e.g. if the wavepacket trajectories are periodic or chaotic, the changes can accumulate, leading to the growth of $(\hat{\delta}, \hat{\zeta})$. This mechanism of inertia-gravity-wave generation can be interpreted as a form of parametric instability. In the next section, we discuss solutions of (3)–(4) and (7)–(9) in simple flows which illustrate the mechanisms just described.

3 Applications to simple flows

We consider three time-independent flows: a vertically sheared, horizontally strained flow, an elliptical flow, and a dipolar flow. We then briefly discuss the behaviour that can be expected in more complex flows with chaotic wavepacket trajectories on the basis of random-strain models.

3.1 Horizontal strain and vertical shear

Perhaps the simplest flow leading to a non-trivial time dependence of \mathbf{k} is a pure strain flow. Here we consider the added effect of a vertical strain and take $\mathbf{U} = (\beta x, -\beta y + \Sigma z, 0)$ for some constants $\beta > 0$ and Σ . We focus on the case $\hat{q} = 0$ and on the long time behaviour, when the wavevector is approximately

$$(k, l, m) \sim (0, e^{\beta t}, \Sigma e^{\beta t} / \beta),$$

up to an irrelevant constant factor. This leads to constant coefficients in (7)–(8) and to a solution $(\hat{\delta}, \hat{\zeta}) \propto \exp(\sigma t)$, where the growth rate σ satisfies

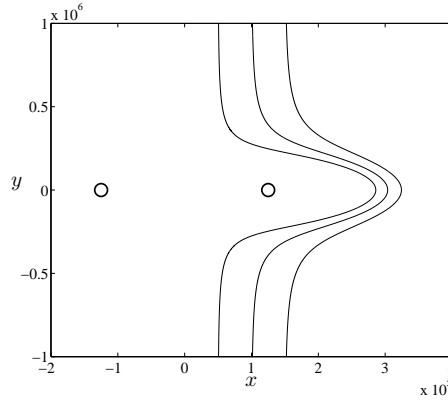
$$2\sigma = \beta \pm \left(\beta^2 - 4 \frac{\Sigma^2 + N^2 \beta^2 / f^2}{\beta^2 + \Sigma^2} \right)^{1/2}.$$

Thus the divergence and vertical vorticity $(\hat{\delta}, \hat{\zeta})$ of the wavepacket increases exponentially. Their growth rate is however less than the growth rate β of the wavevector magnitude κ . Still, the unbounded growth of $(\hat{\delta}, \hat{\zeta})$ is significant: in particular it implies the growth of the vertical gradient of the density and the ultimate breaking of the wavepacket (cf. [4]).

3.2 Elliptical flow

The parametric instability associated with periodic fluctuations of \mathbf{k} is illustrated by the uniform-vorticity elliptical flow $\mathbf{U} = (ay, -by, 0)$, where a and b are constants satisfying $ab > 0$. The instability of this flow is an example of elliptical instability [10], here of a rotating stratified fluid. Equations (7)–(8) have periodic coefficients, and their stability can be analysed using Floquet theory. Numerical and explicit results in the limit of small eccentricity $|a/b - 1| \ll 1$ have been obtained by several authors [10, 13, 12]. They indicate that perturbations whose wavenumber satisfy some resonance conditions grow. In the presence of rotation and stratification, the growth rates decrease rapidly, however. More specifically, for $N > f$, the growth rates can be shown to be exponentially small in the Rossby number \sqrt{ab}/f . They never vanish, so that elliptical flows, both anticyclonic ($ab > 0$) and cyclonic ($ab <$

Fig. 1 Trajectories of three wavepackets in the flow generated by a quasi-geostrophic dipole. The location of the two point vortices is indicated by circles. The wavepackets, which travel in the plane $z = 0$ of the dipole, are characterised by their distance $d = 50, 100$ and 150 km from the axis of the dipole as $t \pm \infty$.



0) are unstable, albeit in exponentially narrow bands of wavenumbers (see [2] for asymptotic estimates of the growth rates). Qualitatively, the same conclusions are expected to hold for all time-independent flows with closed particle trajectories and hence closed wavepacket trajectories.

3.3 Dipole

To illustrate the spontaneous generation of inertia-gravity waves by wavepackets with $\hat{q} \neq 0$, we consider the evolution of a wavepacket in the simple flow corresponding, in the three-dimensional quasi-geostrophic approximation, to a dipole. (This flow is only a solution of the fluid equations in the limit of large f and N , but we use it as a crude model since we expect the qualitative properties of the wavepacket evolution to be insensitive to the details of the flow.) The potential vorticity of the dipole is $Q = \kappa(\delta(x-L) + \delta(x+L))\delta(y)\delta(z)$, with the separation of the point vortices chosen to be $2L = 250$ km. The strength κ was taken such that the propagation speed of the dipole is 10 m s^{-1} . It is convenient to think of this dipole as arrested by a uniform flow; wavepackets located at large distances from the dipole in the y -direction are then swept past the dipole and experience a transient change of wavevector. Figure 1 shows the corresponding trajectories in the (x, y) -plane for three wavepackets located at distances $d = 50, 100$ and 150 km from the dipole axis as $|t| \rightarrow \pm\infty$. Since the flow is uniform for $t \rightarrow \pm\infty$, we can use the exact solution (10) to decompose the perturbation into a vortical mode and two inertia-gravity waves for $|t|$ large. For $t \rightarrow -\infty$, we assume that only the vortical mode is excited. As a result of the transient activity, the inertia-gravity-wave modes are excited and their amplitude $A(t)$ becomes simply $A(t) \sim A_\infty \exp(\pm i\omega_1 t)$ as $t \rightarrow \infty$. The constant A_∞ is therefore an appropriate measure of the spontaneous generation that occurs.

We report results obtained for a wavepacket with $m/\sqrt{k^2 + l^2} \approx 10$ located in the plane $z = 0$ of the dipole. The other relevant parameters are $f = 10^{-4} \text{ s}^{-1}$ and

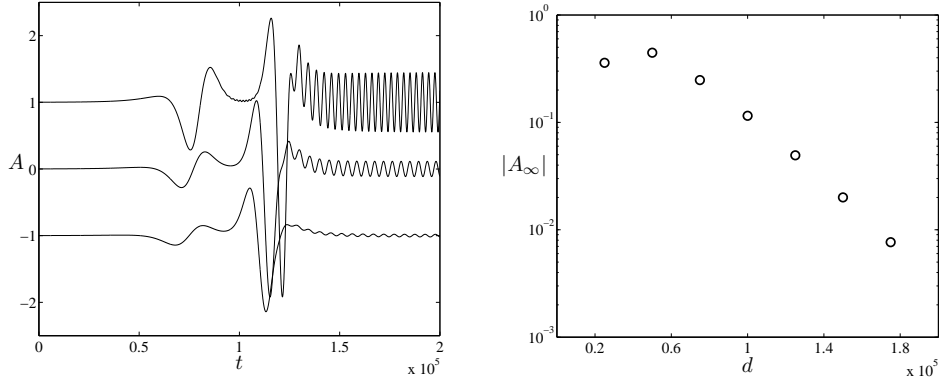


Fig. 2 Inertia-gravity waves generated spontaneously as vortical-mode wavepackets are swept past a dipole. The left panel shows the amplitude of one of the two inertia-gravity-wave mode as a function of time for wavepackets located at distances $d = 25, 50$ and 100 km (from top to bottom curves) of the dipole axis as $t \rightarrow \pm\infty$. The top and bottom curves are offset by ± 1 unit in the A -direction. The right panel shows the amplitude of the inertia-gravity-wave mode as $t \rightarrow \infty$ as a function of the distance d of the wavepacket to the dipole axis.

$N = 10^{-2} \text{ s}^{-1}$. Figure 2 shows results obtained for the different values of the distance d of the wavepacket to the dipole axis. The left panel shows the amplitude of the inertia-gravity-wave component of the flow (obtained by projecting (δ, ξ, \hat{q}) on one of the inertia-gravity-wave mode) for $d = 25, 50$ and 100 km. It demonstrates clearly the appearance of fast oscillations that follows the transient behaviour associated with the encounter with the dipole. It also illustrates the strong dependence of the inertia-gravity-wave amplitude on d which can be thought of as a proxy for an inverse Rossby number. The right panel of Figure 2 shows the magnitude of the amplitude A_∞ that characterises the inertia-gravity waves for $t \rightarrow \infty$. It uses linear–logarithmic coordinates to demonstrate the exponential dependence of A_∞ on d and hence on the inverse Rossby number. Note that an exponential-asymptotics analysis similar to that of Ref. [22] could be carried out to obtain an explicit approximation for A_∞ .

3.4 Random-strain models

As is well known from the study of particle advection, the trajectories of particles and hence wavepackets are typically chaotic when the velocity field is time dependent. The Lagrangian time dependence of the strain $\nabla\mathbf{U}$ that appears on the right-hand side of (4) is therefore very complicated; it is natural to model it by a stationary random process. This is the key idea of the random-strain models proposed by Kraichan [11] in the context of passive-scalar advection (the scalar-concentration gradient obeys (4)). Haynes and Anglade [9] considered random-strain models adapted to the layerwise two-dimensional nature of geophysical flows and concluded that

while, typically, $\kappa \rightarrow \infty$, the aspect ratio $m/\sqrt{k^2 + l^2}$ reaches a stationary distribution. Since this ratio together with $\nabla \mathbf{U}$ determine the coefficients of (7)–(8) for $\hat{q} = 0$ for random-strain models, these equations are essentially those of a linear oscillator with stationary random coefficients. This observation makes it possible to draw some conclusion about the behaviour of $(\hat{\delta}, \hat{\zeta})$. First, these quantities typically grow exponentially, with a deterministic growth rate defined by $\lim_{t \rightarrow \infty} t^{-1} \log |\zeta|$, say, that can be recognised as the Lyapunov exponent of the system. Second, in the limit of small Rossby number, naturally defined using the correlation time of the random process determining the oscillator frequency, the growth rate can be expected to depend crucially on the smoothness of this process. Specifically, the explicit results available for closely related problems [1, 6], suggest that the growth rate is proportional to the power spectrum of the random process evaluated at twice the average oscillator frequency. In the small-Rossby-number limit this average frequency is in the tail of the spectrum and hence entirely controlled by the smoothness of the process. In particular, if the process is real-analytic, the growth rate will be exponentially small in the Rossby number. Thus spontaneous inertia-gravity-wave generation is predicted by random-strain models to have a similar Rossby-number dependence in complex flows as in simple steady flows. The key assumption, which may not always be satisfied, is that the Lagrangian time series of $\nabla \mathbf{U}$ is real-analytic. Note that a simple model for which analytic progress is possible would take $\nabla \mathbf{U}$ to be a white noise so as to apply the techniques developed for the Kazantsev–Kraichnan models of kinematic dynamo and passive-scalar advection (see, e.g., [5, 14] and references therein). This would however be appropriate only for flows with correlation times short compared to f^{-1} and to the inverse strain.

4 Discussion

This paper applies the geometric-optics approach to fluid stability (e.g. [7]) in order to study the spontaneous generation of inertia-gravity waves in a variety of flows. This application, which requires introducing the effect of rotation and stratification, is straightforward because of the particular dispersion relation of inertia-gravity waves: since their intrinsic frequency remains $O(1)$ as $|\mathbf{k}| \rightarrow \infty$, the kinematics of short waves is dominated by the Doppler shift, and wavepackets are simply advected by flows like fluid particles. Nine coupled ordinary differential equations govern the dynamics of the wavepackets, with three controlling their amplitude. This implies that the three types of modes that can be identified when \mathbf{U} is uniform – the vortical mode and the two inertia-gravity modes – are strongly coupled. Only when the Lagrangian evolution is slow compared to the inertia-gravity-wave frequency, that is, in the limit of small (Lagrangian) Rossby number, are they asymptotically decoupled. It is interesting to note that the three amplitude equations then form a two-time-scale system with the same structure as the complete (partial differential) fluid equations [25]. The general conclusions that can be drawn for these system apply, and the generation of inertia-gravity waves, either through spontaneous con-

version of the vortical modes or through unbalanced instabilities, is exponentially weak in the Rossby number. The simple models discussed in this paper make this explicit.

The key interest of the geometric-optics approach is that it makes it possible to examine the growth of perturbations to solutions of partial-differential equations by solving ordinary differential equations. (See Refs. [19, 15] for an alternative approach, namely the pressureless approximation, which also leads to ordinary differential equations.) Here we have considered highly idealised flows for which the velocity field can be written in closed form. This is not necessary, and our future work will implement the solutions of the amplitude equations (7)–(9) for more complex flows obtained from numerical simulations. It will also consider the scaling $f, N = O(\mu^{-1})$ for which the intrinsic frequency is of the same order as the Doppler shift; in this case interactions between the vortical and inertia-gravity modes remain possible, but they are exponentially small in μ .

Acknowledgements The authors are supported by the UK Natural Environment Research Council through a studentship (JMA) and a research grant (JV), and by the EPSRC Network ‘Wave–Flow Interactions’. JV thanks the organisers of the IUTAM workshop ‘Rotating Stratified Turbulence in the Atmosphere and Oceans’ for a stimulating meeting.

References

- [1] Arnold, L., Papanicolaou, G., Wihstutz, V.: Asymptotic analysis of the Lyapunov exponent and rotation number of the random oscillator and applications. *SIAM J. Appl. Math.* **46**, 427–450 (1986)
- [2] Aspden, J.M., Vanneste, J.: Elliptical instability of a rapidly rotating, strongly stratified fluid. *Phys. Fluids* (2009). Submitted
- [3] Badudin, S.I., Shrira, V.I.: On the irreversibility of internal waves dynamics due to wave trapping by mean flow inhomogeneities. part 1. local analysis. *J. Fluid Mech.* **251**, 221–53 (1993)
- [4] Bühler, O., McIntyre, M.E.: Wave capture and wave–vortex duality. *J. Fluid Mech.* **534**, 67–95 (2005)
- [5] Falkovich, G., Gawędzki, K., Vergassola, M.: Particles and fields in fluid turbulence. *Rev. Modern Phys.* **73**(4), 913–975 (2001)
- [6] Figotin, A., Pastur, L.: *Spectra of Random and Almost-Periodic Operators*. Springer (1992)
- [7] Friedlander, S.J., Lipton-Lifschitz, A.: Localized instabilities in fluids. In: S. Friedlander, D. Serre (eds.) *Handbook of Mathematical Fluid Dynamics*, vol. II, pp. 289–353. Elsevier Science (2003)
- [8] Guimbard, D., Leblanc, S.: Local stability of the Abrashkin–Yakubovich family of vortices. *J. Fluid Mech.* **567**, 91–110 (2006)
- [9] Haynes, P.H., Anglade, J.: The vertical-scale cascade in atmospheric tracers due to large-scale differential advection. *J. Atmos. Sci.* **54**, 1121–1136 (1997)

- [10] Kerswell, R.R.: Elliptical instability. *Ann. Rev. Fluid Mech.* **34**, 83–113 (2002)
- [11] Kraichnan, R.H.: Convection of a passive scalar by a quasi-uniform random straining field. *J. Fluid Mech.* **64**, 737–762 (1974)
- [12] McWilliams, J.C., Yavneh, I.: Fluctuation growth and instability associated with a singularity of the balance equations. *Phys. Fluids* **10**, 2587–2596 (1998)
- [13] Miyazaki, T.: Elliptical instability in a stably stratified rotating fluid. *Phys. Fluids A* **5**, 2702–2709 (1993)
- [14] Nazarenko, S., West, R.J., Zaboronski, O.: Fourier space intermittency of the small-scale turbulent dynamo. *Phys. Rev. E* **68**, 026,311 (2003)
- [15] Ngan, K., Straub, D.N., Bartello, P.: Three-dimensionalization of freely-decaying two-dimensional turbulence. *Phys. Fluids* **16**, 2918–2932 (2004)
- [16] Ólafsdóttir, E.I., Olde Daalhuis, A.B., Vanneste, J.: Inertia-gravity-wave radiation by a sheared vortex. *J. Fluid Mech.* **596**, 169–189 (2008)
- [17] Plougonven, R., Snyder, C.: Gravity waves excited by jets: propagation versus generation. *Geophys. Res. Lett.* **32**, L18,802 (2005)
- [18] Snyder, C., Muraki, D., Plougonven, R., Zhang, F.: Inertia-gravity waves generated within a dipole vortex. *J. Atmos. Sci.* **64**, 4417–4431 (2007)
- [19] Straub, D.N.: Instability of 2D flows to hydrostatic 3D perturbations. *J. Atmos. Sci.* **60**, 79–87 (2003)
- [20] Vanneste, J.: Inertia-gravity-wave generation by balanced motion: revisiting the Lorenz-Krishnamurthy model. *J. Atmos. Sci.* **61**, 224–234 (2004)
- [21] Vanneste, J.: Exponential smallness of inertia-gravity-wave generation at small Rossby number. *J. Atmos. Sci.* **65**, 1622–1637 (2008)
- [22] Vanneste, J., Yavneh, I.: Exponentially small inertia-gravity waves and the breakdown of quasi-geostrophic balance. *J. Atmos. Sci.* **61**, 211–223 (2004)
- [23] Viúdez, A.: Spiral patterns of inertia-gravity waves in geophysical flows. *J. Fluid Mech.* **562**, 73–82 (2006)
- [24] Viúdez, A.: The origin of the stationary frontal wave packet spontaneously generated in rotating stratified vortex dipoles. *J. Fluid Mech.* **593**, 359–383 (2007)
- [25] Warn, T., Bokhove, O., Shepherd, T.G., Vallis, G.K.: Rossby number expansions, slaving principles, and balance dynamics. *Quart. J. R. Met. Soc.* **121**, 723–739 (1995)